Optogenetic control of *Drosophila* using a red-shifted channelrhodopsin reveals experience-dependent influences on courtship

Hidehiko K Inagaki[1,2,4], Yonil Jung[1,2,4], Eric D Hoopfer[1,2], Allan M Wong[1,2], Neeli Mishra[2], John Y Lin[3], Roger Y Tsien[1,3] & David J Anderson[1,2]

Optogenetics allows the manipulation of neural activity in freely moving animals with millisecond precision, but its application in *Drosophila melanogaster* has been limited. Here we show that a recently described red activatable channelrhodopsin (ReaChR) permits control of complex behavior in freely moving adult flies, at wavelengths that are not thought to interfere with normal visual function. This tool affords the opportunity to control neural activity over a broad dynamic range of stimulation intensities. Using time-resolved activation, we show that the neural control of male courtship song can be separated into (i) probabilistic, persistent and (ii) deterministic, command-like components. The former, but not the latter, neurons are subject to functional modulation by social experience, which supports the idea that they constitute a locus of state-dependent influence. This separation is not evident using thermogenetic tools, a result underscoring the importance of temporally precise control of neuronal activation in the functional dissection of neural circuits in *Drosophila*.

D. melanogaster is one of the most powerful model organisms available for the genetic dissection of neural circuit function[1,2]. Likewise, the use of light-sensitive microbial opsins, such as channelrhodopsin, has revolutionized the functional dissection of neural circuits in behaving animals[3,4]. Unfortunately, with the exception of larval neurons and peripheral sensory neurons in adults[5–13], this powerful technology and model organism have been largely incompatible in the case of adult flies (but see refs. 10,13). Therefore, *Drosophila* researchers have, to a large extent, been unable to exploit the rapidly expanding optogenetic toolkit for neural circuit manipulation. Although P2X2, an ionotropic purinergic receptor, has been used as an optogenetic tool in adult *Drosophila*, this technique requires injection of caged ATP into the brains of individual anesthetized flies[14]. This relatively invasive technology is suboptimal for many applications, especially large-scale, high-throughput screening.

In the absence of facile optogenetic manipulation, dTRPA1, a thermosensitive cation channel, has been the preferred method for neuronal activation in freely behaving adult flies[1,15]. Because this method depends on changes in temperature to control neuronal activity, however, it lacks precision in both the temporal and intensity domains and suffers from potentially confounding influence of temperature changes on behavior.

Here we demonstrate that expression of ReaChR in adult central nervous system (CNS) neurons enables rapid and temporally precise control of behavior in freely moving adult *Drosophila*. Using this optogenetic method, we have separated the control of wing extension, a male-specific courtship behavior, into either probabilistic, state-dependent or deterministic, command-like components. Moreover, by combining ReaChR activation with functional calcium imaging, we have also identified a neural correlate of the influence of social experience on male courtship behavior.

RESULTS

Optogenetic vs. thermogenetic control of gustatory neurons

We reasoned that previously described channelrhodopsin-2 (ChR2) variants do not work well in adult *Drosophila* owing, at least in part, to low penetrance of blue light through the cuticle. Indeed, direct measurements *in vivo* indicated that the penetrance of blue light through the cuticle is much weaker (~1%) than that of longer wavelengths such as green or red light (5–10%) (**Fig. 1a**). Therefore, we created transgenic flies that express the recently developed red-shifted channelrhodopsins, C1V1(T/T)[16] and ReaChR[17] under the control of the Gal4–upstream activating sequence (UAS) system, to test whether red-shifted light can penetrate the cuticle sufficiently to activate neurons expressing these channels (see **Supplementary Table 1** for a listing of all transgenic fly strains created).

We first compared the efficacy of different opsins to activate sugar-sensing gustatory receptor neurons (GRNs) that express the receptor Gr5a[18]. Optogenetic activation of Gr5a neurons using ChR2 has previously been shown to trigger the proboscis extension reflex (PER) in *Drosophila*[6,12] (**Supplementary Video 1**). All of the blue light–sensitive opsin variants tested (ChR2 (refs. 19,20),

[1]Howard Hughes Medical Institute, Pasadena, California, USA. [2]Division of Biology, California Institute of Technology, Pasadena, California, USA. [3]Department of Pharmacology, University of California, San Diego, La Jolla, California, USA. [4]These authors contributed equally to this work. Correspondence should be addressed to D.J.A. (wuwei@caltech.edu).

RECEIVED 3 AUGUST; ACCEPTED 18 NOVEMBER; PUBLISHED ONLINE 22 DECEMBER 2013; DOI:10.1038/NMETH.2765

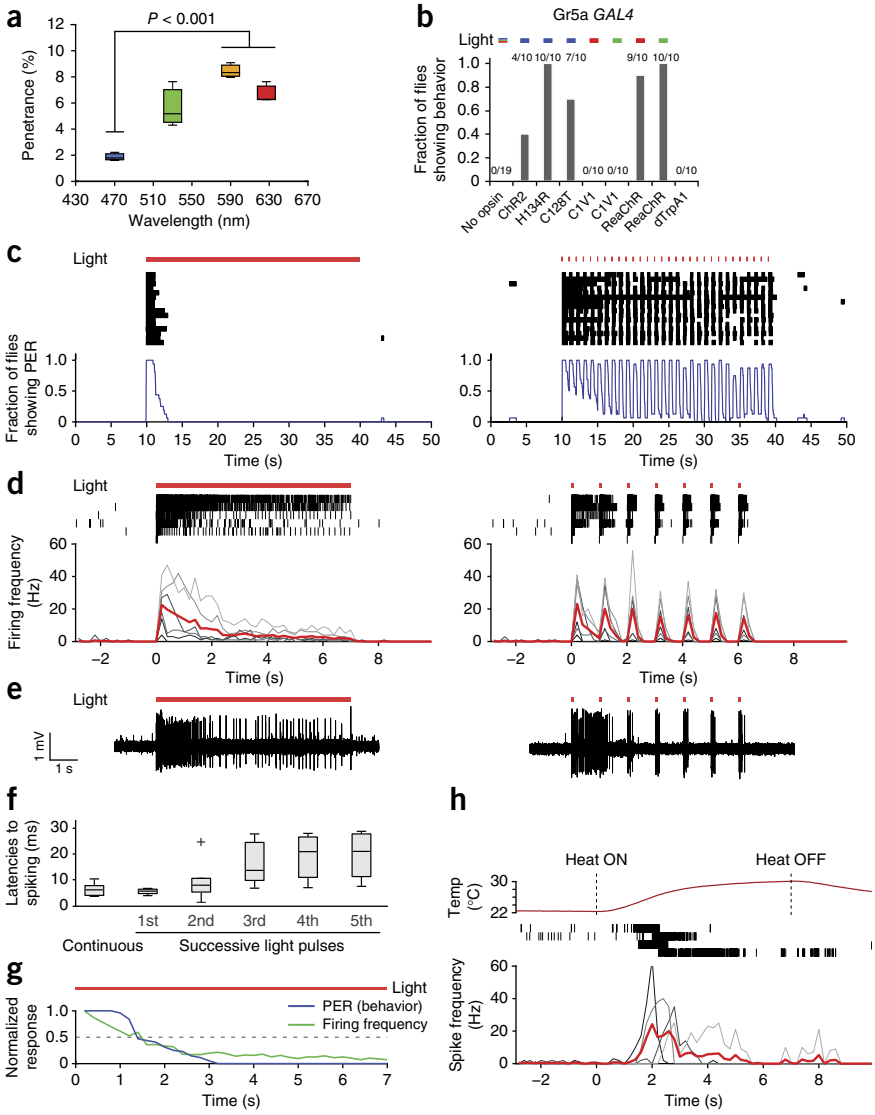

Figure 1 | Optogenetic versus thermogenetic control of Gr5a GRNs. (**a**) Penetrance of light through the adult fly cuticle. $n = 3$. $P = 0.0046$ for one-way ANOVA followed by t-test with Bonferroni correction ($P < 0.001$). (**b**) Fraction of flies showing PER triggered by different opsins expressed in Gr5a GRNs. Fractions indicate the number of responders out of the number of flies tested. Activation wavelengths are represented as blue (470 nm), green (530 nm) and red (627 nm) bars. For the no-opsin control, all the wavelengths were tested. (**c**–**e**) Behavioral (**c**) and electrophysiological (**d**,**e**) responses of flies expressing ReaChR in Gr5a GRNs. Red lines (**c**–**e**) represent the photostimulation pattern (627 nm, 1.1 mW/mm^2); pulsed photostimulation (right) was delivered at 1 Hz (100-ms pulse width). In **c**, raster plots show PER bouts, and blue curves show the fraction of flies showing PER (time bins: 1 s; $n = 16$). In **d**, raster plots show Gr5a GRNs spikes; the lower plots show average spiking rate (red) and spiking rates for individual flies (gray; time bins, 200 ms; $n = 6$). (**e**) Sample traces. (**f**) Latencies to first spike following photostimulation onset from **d**. Box plot whiskers represent 1.5× interquartile range of the lower and upper quartiles; box limits indicate lower quartile, median and upper quartile, from bottom to top; "+" indicates outlier data beyond the whiskers. (**g**) Overlay of normalized PER and firing frequencies during continuous photostimulation based on **c**,**d**. (**h**) Top, measured temperature change caused by a heat source placed near the labellum. Center, plots representing spikes in Gr5a GRNs expressing dTrpA1. Bottom, spiking responses plotted as in **d**; $n = 4$.

H134R (ref. 21) and C128T (ref. 22)) induced PER behavior in response to photostimulation at 470 nm, although only H134R yielded responses in 100% of flies (**Fig. 1b**). Flies expressing ReaChR in Gr5a GRNs yielded robust PER responses to both red (627 nm) and green (530 nm) light. In contrast, flies expressing C1V1(T/T) did not exhibit PERs in response to either red or green light (**Fig. 1b**). Instead, they moved their proboscis slightly, albeit in a manner time locked to photostimulation, suggesting that C1V1(T/T) has only a weak ability to activate Gr5a GRNs.

Surprisingly, in flies expressing dTrpA1 in Gr5a GRNs, we did not observe any behavioral response at an ambient temperature known to activate the ion channel (32 °C)[8,15] (**Fig. 1b**) or during gradual ramping to this temperature from 22 °C (data not shown). Interestingly, activation of dTrpA1 in Gr5a GRNs using heat pulses from an infrared (IR) laser[23] has been reported to induce a PER. Upon continuous current injection, some neurons develop a depolarization block[24]. We reasoned that if Gr5a neurons are continuously or gradually activated via TrpA1, they may undergo a rapid depolarization block that prevents PER behavior. Consistent with this idea, continuous illumination of Gr5a-ReaChR flies produced only a transient PER reaction (half-time for decay, 1.5 s), whereas pulsatile illumination (1 Hz, 100-ms pulse duration) evoked a train of PERs time locked to each light pulse (**Fig. 1c** and **Supplementary Video 1**).

Consistent with this result, electrophysiological recording of Gr5a GRNs revealed that pulsed light caused continuous bursts of spiking throughout the stimulation period (**Fig. 1d**,**e**) with short latencies (**Fig. 1f**). In contrast, spiking activity decayed exponentially during continuous light stimulation (half-time for decay, ~1.5 s; **Fig. 1d**,**e**). The rapid decay of both spiking and PER behavior during continuous activation of ReaChR (**Fig. 1g**; Pearson's correlation coefficient, $r = 0.96$) suggests that the former likely accounts for the latter.

Similar to the results obtained using continuous ReaChR activation, TrpA1 activation triggered only transient spiking in Gr5a GRNs, with a strong decay after several seconds (**Fig. 1h**). Together, these data may explain why PER responses were not induced by constitutive or gradual thermal activation in Gr5a-TrpA1–expressing flies (**Fig. 1b**). They also reconfirm the importance of pulsed activation of neurons to avoid depolarization block, as reported previously in other systems[4] (but note that depolarization block does not occur in all neuronal subtypes[8]).

Activation of CNS neurons with ReaChR

Only a few studies have reported successful elicitation of behavior in adult *Drosophila* by activating CNS neurons expressing blue

light–sensitive opsins[10,13]. To determine whether activation using ReaChR would be more effective, we directly compared the behavioral responses of flies expressing blue light– and red light–sensitive opsins in *GAL4* lines driving expression in different populations of CNS neurons. These lines included *hb9* (*exex*)-*GAL4* (ref. 25), whose activation induces side walking (**Supplementary Video 2**) and, at higher intensities, paralysis (loss of postural control and immobility); *Corazonin* (*Crz*)-*GAL4*, whose activation induces abdominal bending and ejaculation[26] (**Supplementary Video 3**); *fru*-*GAL4* (ref. 27), which labels ~1,500 neurons throughout the brain and whose activation in males induces mating behavior including wing extension[28] and abdominal bending, and at higher intensities, paralysis is observed (**Supplementary Video 4**); and P1-*GAL4*, a 'split' *GAL4* (refs. 29,30) driver generated from parental *GAL4* lines[31] identified in a behavioral screen (E.D.H. and D.J.A., unpublished data) that is specifically expressed in ~16–20 male-specific P1 neurons and whose activation elicits wing extension in males in the absence of females[28,32] (**Supplementary Video 5**). To facilitate the control and monitoring of light-induced behaviors in freely moving adult flies in a high-throughput, cost-effective and flexible manner, we developed a high-power LED–based activation system (**Fig. 2a–c**; **Supplementary Fig. 1**, **Supplementary Table 2**, **Supplementary Software** and Online Methods).

Strikingly, among all five opsins tested using these CNS drivers, ReaChR was the only one whose activation yielded robust behavioral phenotypes in a light-dependent manner (**Fig. 2d**). The evoked behaviors were not due to innate responses to light: control flies lacking UAS-ReaChR did not exhibit them in response to all the wavelengths tested (**Fig. 2d**). The fact that blue light–activated opsins yielded a behavioral response (PER) when expressed in GRNs but not in the CNS neurons tested here likely reflects the fact that the peripheral GRNs are located close to the cuticle, where blue light may penetrate more easily. Analysis of C1V1(T/T) expression in CNS neurons revealed that this opsin is expressed weakly in cell somata and not trafficked to arborizations, whereas ReaChR is strongly expressed in somata and is trafficked to arborizations as well (**Supplementary Fig. 2a**). This difference likely accounts for the different efficacies of the two red-shifted opsins in this system.

The peak of the ReaChR action spectrum (measured in cultured hippocampal neurons) is ~590 nm (ref. 17). The efficacy of ReaChR activation by different wavelengths in freely behaving flies will, however, reflect a combination of factors including cuticular penetration and intensity as well as proximity to peak sensitivity. To empirically determine the optimal wavelength of light for behavioral assays, therefore, we compared the ability of blue (470-nm), green (530-nm), amber (590-nm) and red (627-nm) light to induce behavior in flies expressing ReaChR under the control of different CNS *GAL4* drivers. When not normalized for intensity, green LEDs had the strongest capacity to elicit ReaChR-dependent behaviors (**Fig. 2d**,**f**,**g**). In some cases (pIP10 neurons; see below), robust behavioral responses were detected only using green light and hardly at all using other wavelengths. Although amber light is closest to the peak of the ReaChR action spectrum, commercial LEDs of this wavelength are dimmer than the others and therefore did not elicit strong behavioral responses (**Fig. 2f**,**g**).

Although TrpA1-mediated activation of P1 neurons can elicit wing extension[28,32], in our direct comparison the fraction of solitary male flies showing a wing extension phenotype was much higher using ReaChR and green light than using TrpA1 (**Fig. 2d**). This suggests that the intensity of activation obtained using ReaChR (and green light) can be substantially stronger than that achieved using dTrpA1, without subjecting flies to the high temperatures necessary to activate the latter. Nevertheless, although green LEDs elicited the strongest behavioral responses, flies can see this wavelength, whereas their sensitivity to wavelengths >620 nm is much lower[33,34] (see, however, ref. 35). Therefore, we used red LEDs whenever possible to avoid behavioral artifacts caused by strong visual stimulation.

To investigate whether the strength of a given ReaChR-dependent behavioral phenotype can be quantitatively tuned, we tested multiple frequencies and intensities of light pulses using the P1-*GAL4* driver (pulse width, 5 ms). There was a frequency-dependent increase in the fraction of flies showing wing extension as well as in the average number and duration of wing extension bouts per fly (**Fig. 2e** and **Supplementary Fig. 2e**), even when we corrected for the total duration of illumination (**Supplementary Fig. 2f**). The *hb9*-*GAL4* and *fru*-*GAL4* drivers also yielded an increase in the fraction of flies showing the respective behavioral responses as the intensity was increased, albeit over different ranges (**Fig. 2f**,**g**). Together these data indicate that ReaChR can be used to tune behavioral phenotypes by varying the light intensity and/or pulse frequency, over a relatively broad dynamic range.

Probabilistic vs. deterministic control of wing extension

Previous studies of the neural circuitry underlying male courtship behavior in *Drosophila* have used neuronal activation methods, including P2X2 and TrpA1, to identify different neuronal subclasses that control courtship song[28,32,36,37]. In particular, studies using TrpA1 have described two neuronal classes in the central brain controlling this behavior: one, called P1 or pMP4, constitutes a population of interneurons[28,32,37], and the other, called pIP10, constitutes a small group of descending neurons that project to the ventral nerve cord[28] (**Fig. 3b**). The presynaptic terminals of P1 neurons overlap with the dendrites of pIP10 neurons, which suggests that they may be synaptic partners[28]; however, the difference, if any, between the roles of these neurons in controlling courtship song has not been apparent, as similar behaviors are evoked by TrpA1-mediated stimulation of both classes[28].

We used the time-resolved control of neuronal activation afforded by ReaChR to compare the temporal patterns of stimulation-evoked behavioral responses in P1 versus pIP10 neurons. To express ReaChR in the latter cells, we used an intersectional strategy combining a specific *GAL4* line (VT40556; ref. 28) with *fru*-*FLP*[38] and a UAS>mCherry>ReaChR transgene (where ">" denotes *FRT* sites, the target of Flp recombinase; see **Supplementary Fig. 2b**,**c** and **Supplementary Table 1**). Anatomical analysis using a Citrine reporter fused to the C terminus of ReaChR confirmed the restricted expression of ReaChR in flies of the appropriate intersectional genotype (**Supplementary Fig. 2d**).

Surprisingly, we found that the temporal dynamics of wing extension evoked by activation of P1 and pIP10 neurons were strikingly different. ReaChR-mediated activation of P1 neurons evoked wing extension in a probabilistic or stochastic manner: the initiation of wing extension was not time locked to the onset of illumination but rather occurred with variable latencies

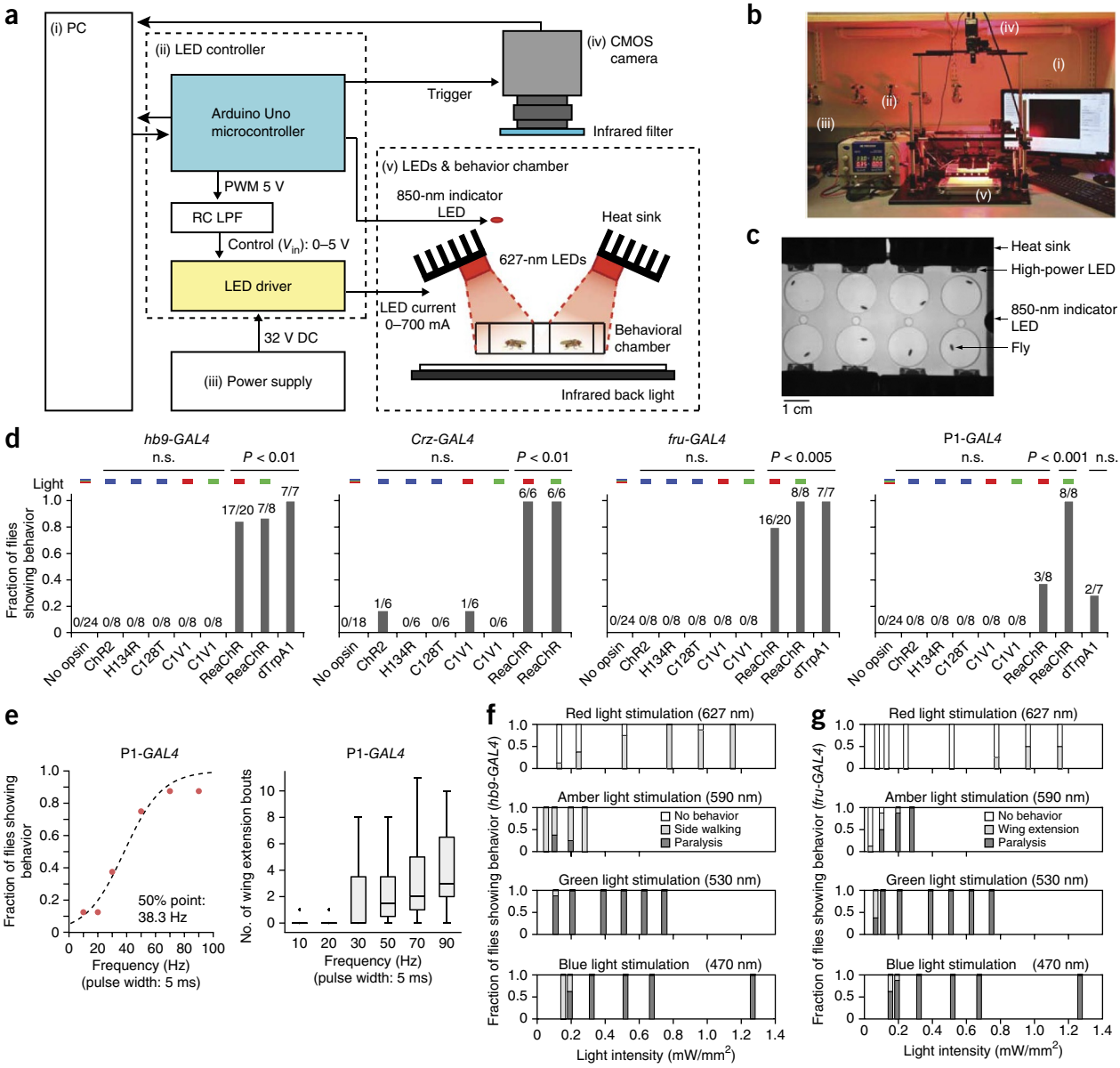

Figure 2 | ReaChR enables light-dependent activation of CNS neurons in *Drosophila*. (**a**,**b**) Experimental setup for high-power LED–based activation system. Each roman numeral in the diagram (**a**) corresponds to that in the photograph (**b**) (see **Supplementary Fig. 1** and **Supplementary Table 2**). PWM, pulse-width modulation; RC LPF, resistor-capacitor low-pass filter; CMOS, complementary metal-oxide semiconductor. (**c**) View from the CMOS camera. (**d**) Comparison of behavioral responses of flies expressing different channelrhodopsin variants in distinct CNS subpopulations. Plot properties are as in **Figure 1b**. "Fraction of flies showing behavior" indicates side-walking or knockout phenotype (*hb9-GAL4*), ejaculation (*Crz-GAL4*), wing extension or knockout (*fru-GAL4*), or wing extension (P1-*GAL4*). "No opsin" is the empty promoter *GAL4* (BFP-*GAL4*; Online Methods) crossed with UAS-ReaChR. Flies showing any of the characteristic behaviors during 1 min of continuous photostimulation were scored as responders. *P* values represent Fisher's exact test with Bonferroni correction (comparing no-opsin control with each column). *P* values for significant columns in **d**, from left to right and each $\times 10^{-4}$, are 4.3, 56, 12, 77, 77, 13, 6.2, 12 and 6.2. n.s., not significant. (**e**) ReaChR-mediated activation of P1 neurons using different frequencies of red light pulses (627 nm, 1.1 mW/mm^2, 1 min) (P1-*GAL4*; UAS-ReaChR(attP40)). The fraction of flies showing wing extension during 1-min photostimulation trials was fitted by a sigmoidal function to calculate the 50% point. $n = 8$. Box plots properties are as in **Figure 1f**. (**f**,**g**) Fraction of flies exhibiting characteristic behaviors at different photostimulation intensities and wavelengths, in animals expressing *hb9-GAL4* (**f**) or *fru-GAL4* (**g**) and UAS-ReaChR. $n = 8$.

throughout the stimulation period (17.7 ± 27.5 s (mean ± s.d.); **Fig. 3a**,**c**). The average duration of each bout was short (0.99 ± 0.48 s) relative to the duration of photostimulation (30 s). Finally, the termination of the behavior was not time locked to the termination of stimulation; rather, we observed persistent wing extension bouts in the intervals between photostimulation trials (**Fig. 3a**,**e**; Pearson's correlation coefficient between stimulation pattern and behavioral response, $r = 0.004$).

In contrast to the results observed with P1 neurons, activation of pIP10 neurons triggered robust wing extension in a deterministic manner (**Fig. 3a** and **Supplementary Video 5**). The onset of the behavior was strongly time locked to the onset of stimulation, with a very short latency (0.08 ± 0.04 s; **Fig. 3a**,**c**). Once initiated, wing extension continued throughout the photostimulation period and terminated, with few exceptions, with the end of photostimulation (**Fig. 3a**,**d**; Pearson's correlation coefficient

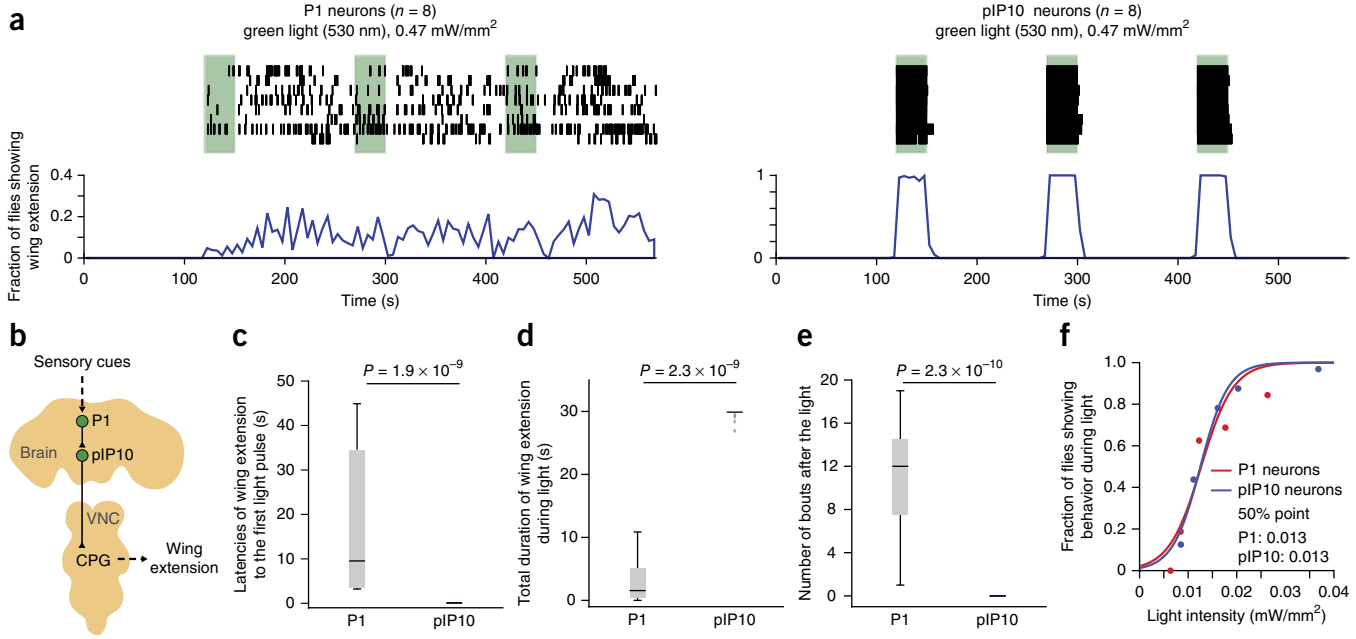

Figure 3 | Probabilistic versus deterministic optogenetic control of courtship song. (**a**) Activation of P1 neurons (P1-*GAL4*; UAS-ReaChR(VK5)) (left) and pIP10 neurons (VT40556/UAS>mCherry>ReaChR(attP40); *fru-FLP*) (right) with green light (530 nm, 0.47 mW/mm^2). Top, raster plot representing wing extension bouts (n = 8 flies per genotype). Green bars represent 30-s continuous photostimulation trials with 120-s intertrial intervals. Bottom, fraction of flies showing wing extension (time bins, 5 s). Note the different y-axis scales. P1 responses during trials 2 and 3 are more clearly phased to the onset of photostimulation at lower light intensities (**Supplementary Fig. 3a**). (**b**) Schematic illustrating neuronal circuit control of courtship song, simplified from ref. 28. VNC, ventral nerve cord; CPG, central pattern generator. (**c**) Latency to first wing extension after onset of the first photostimulation. (**d**) Total duration of wing extension during photostimulation. (**e**) Number of wing extension bouts during 30 s following photostimulation termination. Plots in **c**–**e** are based on data in **a**. P values represent Mann-Whitney U tests. Box plots properties are as in **Figure 1f**. (**f**) Fraction of flies showing wing extension during a single photostimulation trial as a function of light intensity (green light: 530 nm, continuous, 30 s). The data were fitted by a sigmoidal function to calculate the 50% point. n = 32 for both P1 neurons and pIP10 neurons.

between stimulation pattern and behavioral response, r = 0.993). With weaker intensities of illumination close to the wing extension response threshold (≤0.012 mW/mm^2), such responses were less efficiently evoked; but responses were still restricted to the photostimulation period, and no persistent behavior between trials was observed (**Supplementary Fig. 3a**).

These differences between P1 and pIP10 neurons in the temporal dynamics of ReaChR activation-evoked wing extensions do not reflect a higher sensitivity of pIP10 neurons relative to P1 neurons because the intensity dependence of pIP10-evoked wing extension by green light was almost identical to that of P1 neurons (**Fig. 3f**). Moreover, these properties were largely independent of illumination intensity (**Figs. 4** and **5**).

Social isolation modulates ReaChR-activated wing extension

The probabilistic or biasing nature of the wing extension responses elicited by ReaChR-mediated activation of P1 neurons suggested that these neurons might encode, or be modified by, state-dependent influences on male courtship behavior. Interestingly, social isolation of male flies for more than several days enhances courtship behavior, including singing, toward females[39]. To investigate whether P1 neurons might be modulated by such experience, we first determined whether social isolation lowers the threshold for eliciting wing extension by using ReaChR-mediated stimulation of these neurons. Indeed, the intensity of red light that evoked wing extension in 50% of flies expressing ReaChR in P1 neurons was lower in males that were socially isolated for 7 d (single housed males, or SH) than in group-housed males (GH; **Fig. 4**). A similar effect was observed using green light (**Supplementary Fig. 3b**). For each of three different parameters measured, socially isolated flies exhibited significantly higher values than group housed flies (**Fig. 4c**). Thus, social isolation effectively 'tuned' the response to ReaChR activation of P1 neurons such that the probability of a wing extension response was increased. These data suggest that the increased sensitivity to ReaChR activation of wing extension occurs in P1 neurons themselves, or in a functionally downstream population.

Because pIP10 neurons are thought to be functionally downstream of P1 neurons[28] (**Fig. 3b**), we investigated whether ReaChR activation of wing extension via these descending neurons was also sensitive to social experience. Because red light was not strong enough to activate wing extension in male flies expressing ReaChR in pIP10 neurons, we used green light to trigger wing extension. Activation of pIP10 neurons using ReaChR did not reveal any differences between singly housed and group-housed flies in the efficiency with which photostimulation evoked wing extension behavior, even at lower intensities that evoked responses in only a subset of flies (**Fig. 5**). These data indicate that the enhanced sensitivity of ReaChR-evoked wing extension in singly housed flies using the P1-*GAL4* driver is likely to occur in P1 neurons themselves (or in other downstream neurons) rather than in pIP10 neurons. They also indicate that the sensitization of the P1 response by social isolation does not reflect a general increase in sensitivity among all neurons involved in wing extension behavior.

Functional calcium imaging combined with ReaChR activation

To examine directly whether social isolation enhances the sensitivity of P1 neurons to ReaChR activation, we performed calcium

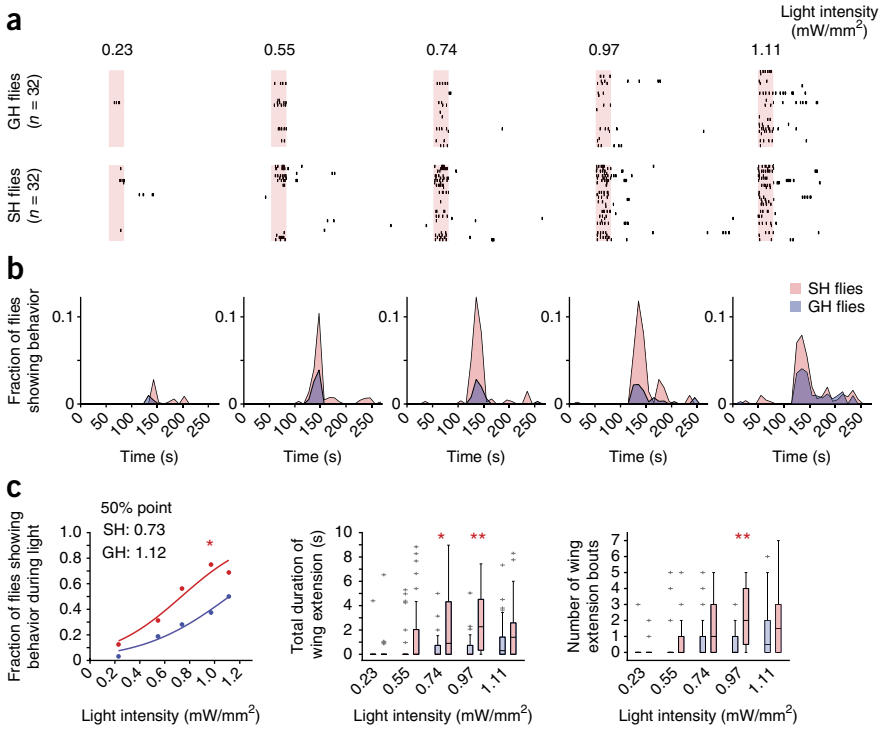

Figure 4 | Social isolation lowers the threshold for ReaChR-activated male courtship behavior. (**a**) Raster plots representing wing extension bouts from group-housed (GH) or singly housed (SH) flies expressing ReaChR in P1 neurons (P1-*GAL4*/UAS-ReaChR(VK5)). Flies were activated with different intensities of red light (627 nm). Light red bars in raster plots indicate photostimulation trials (30 s of continuous light), with different intensities indicated above the bars; $n = 32$ flies per intensity. (**b**) Fraction of flies showing wing extension based on the raster plots in **a**. Data were binned every 10 s. The time scale is the same in **a** and **b**. (**c**) Different parameters extracted from the raster plots in **a**. Properties of box plots are as in **Figure 1f**; "+" indicates outlier data larger than the upper whisker. *P* values were obtained from Friedman's test comparing SH and GH flies ($P = 6.3 \times 10^{-28}$) followed by Fisher's exact test with Bonferroni correction comparing SH and GH flies at each intensity of light (*$P = 0.01$) (**c**, left); Kruskal-Wallis one-way ANOVA followed by Mann-Whitney *U* tests with Bonferroni correction (*$P = 0.027$ and **$P < 0.005$) (**c**, center and right); and Kruskal-Wallis one-way ANOVA $P = 6.4 \times 10^{-11}$ (**c**, center) and $P = 8.2 \times 10^{-12}$ (**c**, right).

imaging experiments in isolated fly brains using laser-scanning two-photon microscopy, taking advantage of the relative separation of the action spectrum peaks for ReaChR and GCaMP3.0 (ref. 40; **Fig. 6a**). Notably, coexpression of GCaMP3.0 in P1 neurons together with ReaChR did not diminish the ability of the latter to mediate light-evoked wing extension in freely moving flies, a result indicating that the calcium-buffering effect of GCaMP3.0 does not interfere with this behavior (data not shown).

An amber LED (590 nm) was used for photostimulation during imaging experiments in order to maximize overlap with the peak of

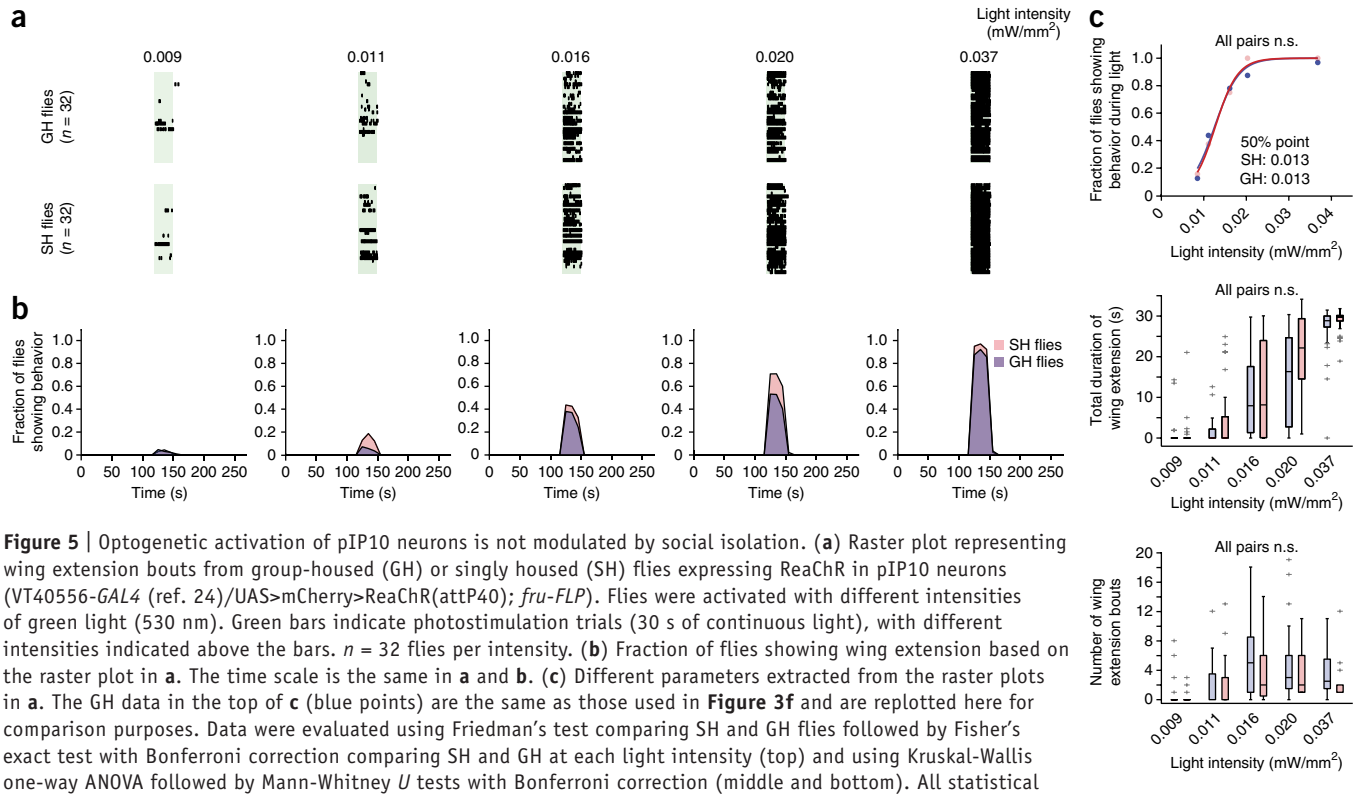

Figure 5 | Optogenetic activation of pIP10 neurons is not modulated by social isolation. (**a**) Raster plot representing wing extension bouts from group-housed (GH) or singly housed (SH) flies expressing ReaChR in pIP10 neurons (VT40556-*GAL4* (ref. 24)/UAS>mCherry>ReaChR(attP40); *fru-FLP*). Flies were activated with different intensities of green light (530 nm). Green bars indicate photostimulation trials (30 s of continuous light), with different intensities indicated above the bars. $n = 32$ flies per intensity. (**b**) Fraction of flies showing wing extension based on the raster plot in **a**. The time scale is the same in **a** and **b**. (**c**) Different parameters extracted from the raster plots in **a**. The GH data in the top of **c** (blue points) are the same as those used in **Figure 3f** and are replotted here for comparison purposes. Data were evaluated using Friedman's test comparing SH and GH flies followed by Fisher's exact test with Bonferroni correction comparing SH and GH at each light intensity (top) and using Kruskal-Wallis one-way ANOVA followed by Mann-Whitney *U* tests with Bonferroni correction (middle and bottom). All statistical tests yielded $P > 0.05$ (n.s., not significant). Properties of box plots are as in **Figure 1f**.

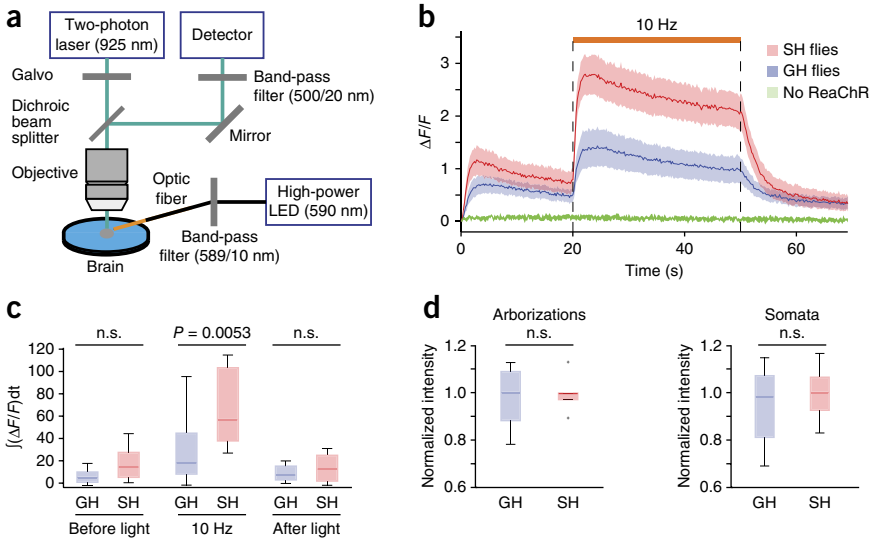

Figure 6 | Functional calcium imaging of P1 neurons. (**a**) Experimental setup for calcium imaging (Online Methods). (**b**) Responses of P1 neurons ($\Delta F/F$, normalized fluorescence change) to ReaChR activation were monitored using two-photon laser-scanning microscopy. Flies expressing both ReaChR and GCaMP3 in P1 neurons (P1-*GAL4*/UAS-ReaChR(attP40); UAS-GCaMP3(VK5)) were singly housed (SH; $n = 11$) or group-housed (GH; $n = 16$) and their brains were imaged. Amber light (590 nm, 1.7 mW/mm^2) with a 5-ms pulse width was delivered at 10 Hz for 30 s (orange line above traces). GCaMP3.0 emissions were monitored in the arborizations of P1 neurons. Flies expressing GCaMP3.0 but not ReaChR in P1 neurons (P1-*GAL4*; UAS-GCaMP3(VK5)) were used as negative controls ($n = 3$). Solid red and blue lines represent average traces, and envelopes indicate s.e.m. (**c**) Quantification of fluorescence changes. $\int(\Delta F/F)dt$, integrated $\Delta F/F$ during 30 s of light activation. Data were analyzed from **b**. n.s., not significant. (**d**) Expression level of ReaChR at the arborizations and somata of P1 neurons were quantified using a Citrine tag fused to the C terminus of ReaChR. *P* values were obtained from Mann-Whitney *U* tests with Bonferroni correction. Box plots properties are as in **Figure 1f**.

the ReaChR action spectrum. Excitation scanning caused an initial increase in baseline GCaMP3.0 fluorescence in fly brains coexpressing ReaChR in P1 neurons, even in the absence of amber light excitation of ReaChR (**Fig. 6b**). These increases were not observed in fly brains lacking UAS-ReaChR, a result implying that they reflect cross-activation of ReaChR by the GCaMP3.0 excitation beam (925 nm). Nevertheless, amber light still evoked a clear increase in the strength of GCaMP3.0 emissions over this background (**Fig. 6b**).

Using these conditions, we compared the GCaMP3.0 response of P1 neurons to ReaChR activation of these same neurons in brains from singly housed and group-housed flies. P1 neurons in SH fly brains showed larger ReaChR-evoked calcium influxes than did GH fly brains (**Fig. 6b**,**c**). Quantitative analysis of ReaChR-Citrine expression in these cells indicated that this difference was not due to higher levels of P1-*GAL4* expression in SH flies (**Fig. 6d**). Together these behavioral and imaging experiments suggest that the excitability of P1 neurons can be modulated by prior social experience. Attempts to monitor calcium transients in pIP10 neurons were precluded by the complex expression pattern and low level of GCaMP3 expression driven by this *GAL4* line.

DISCUSSION

Here we describe a system for optogenetic activation of behavior in freely moving adult flies using ReaChR, a newly described red-shifted opsin[17] (see the **Supplementary Note** for a discussion why ReaChR is more effective than other channelrhodopsins tested). The strength of activation obtained using ReaChR, and the broad dynamic range of intensities and frequencies over which stimulation can be delivered, translates to a more quantitative and temporally controlled approach to investigating the neuronal control of behavior than that provided by available thermogenetic tools (but see ref. 23). The use of ReaChR with red light also reduces the confounding influence of strong visual stimulation that occurs when using blue light–activated opsins or with the temperature increases required by thermogenetic effectors. Finally, the ability to control activation using LEDs, rather than lasers[14,23], permits a relatively inexpensive approach for large-scale, high-throughput screening of behaviors.

Using ReaChR to monitor both behavioral sensitivity and neuronal activation, we discovered that (i) P1 and pIP10 neurons control male courtship song in a state-like (probabilistic and persistent) and command-like (deterministic and time-locked) manner, respectively; and (ii) the effect of social isolation to increase male courtship behavior is mediated, at least in part, through an increase in the excitability of P1 neurons (**Supplementary Table 3**). It has been proposed, on the basis of anatomical data, that P1 neurons are part of a circuit integrating multimodal sensory cues that control courtship behavior[38]. Our observations suggest that P1 neurons also integrate this information with the flies' history of social experience, in a manner that influences the probability that the flies will exhibit courtship behavior. To our knowledge, this represents the first observation of a neural correlate of social experience in *Drosophila*. Interestingly, we did not observe any evidence of persistent calcium transients in P1 neurons after photoactivation, which implies that the persistent wing extension triggered by P1 activation is mediated by other neurons. The mechanisms underlying the influence of social state on P1 excitability, and persistent activity, are interesting topics for future investigation.

Although ReaChR-based activation of behavior was effective in all the *GAL4* lines tested, the optogenetic toolkit in *Drosophila* could benefit from further engineering of red-shifted opsins with a narrower action spectrum and faster kinetics, and also by development of red-shifted variants of inhibitory opsins. Together such tools would further enhance the applicability of optogenetics to neural circuit dissection in *Drosophila*.

METHODS

Methods and any associated references are available in the online version of the paper.

Note: Any Supplementary Information and Source Data files are available in the online version of the paper.

ACKNOWLEDGMENTS

We thank K. Deisseroth (Stanford University) and B. Pfeiffer (Janelia Farm Research Campus) for plasmids. Fly stocks were generously provided by the Bloomington Stock Center, A. Fiala (Georg-August-Universität Göttingen),

G.M. Rubin, L.L. Looger, B.J. Dickson (Janelia Farm Research Campus) and P.A. Garrity (Brandeis University). We also thank members of the Anderson lab for helpful discussion and sharing of flies. H.K.I. was supported by the Nakajima Foundation. J.Y.L. was funded by Foundation of Research, Science and Technology New Zealand. The project was supported by grants from the US National Institutes of Health to R.Y.T. (NS027177) and to D.J.A. (R01DA031389-03). D.J.A. and R.Y.T. are supported by the Howard Hughes Medical Institute.

AUTHOR CONTRIBUTIONS

H.K.I. and D.J.A. designed the experiments. H.K.I., Y.J. and N.M. performed behavioral experiments. H.K.I. and A.M.W. created the transgenic flies. H.K.I. performed physiological experiments. E.D.H. provided P1-*GAL4*. J.Y.L. and R.Y.T. provided the ReaChR reagent and advice on its biophysical properties. H.K.I. and Y.J. performed the data analysis. H.K.I. and D.J.A. prepared the figures and wrote the paper.

COMPETING FINANCIAL INTERESTS

The authors declare no competing financial interests.

1. Venken, K.J., Simpson, J.H. & Bellen, H.J. Genetic manipulation of genes and cells in the nervous system of the fruit fly. *Neuron* **72**, 202–230 (2011).
2. Luo, L., Callaway, E.M. & Svoboda, K. Genetic dissection of neural circuits. *Neuron* **57**, 634–660 (2008).
3. Fenno, L., Yizhar, O. & Deisseroth, K. The development and application of optogenetics. *Annu. Rev. Neurosci.* **34**, 389–412 (2011).
4. Yizhar, O., Fenno, L.E., Davidson, T.J., Mogri, M. & Deisseroth, K. Optogenetics in neural systems. *Neuron* **71**, 9–34 (2011).
5. Schroll, C. *et al.* Light-induced activation of distinct modulatory neurons triggers appetitive or aversive learning in *Drosophila* larvae. *Curr. Biol.* **16**, 1741–1747 (2006).
6. Zhang, W., Ge, W. & Wang, Z. A toolbox for light control of *Drosophila* behaviors through Channelrhodopsin 2-mediated photoactivation of targeted neurons. *Eur. J. Neurosci.* **26**, 2405–2416 (2007).
7. Suh, G.S. *et al.* Light activation of an innate olfactory avoidance response in *Drosophila*. *Curr. Biol.* **17**, 905–908 (2007).
8. Pulver, S.R., Pashkovski, S.L., Hornstein, N.J., Garrity, P.A. & Griffith, L.C. Temporal dynamics of neuronal activation by Channelrhodopsin-2 and TRPA1 determine behavioral output in *Drosophila* larvae. *J. Neurophysiol.* **101**, 3075–3088 (2009).
9. Gordon, M.D. & Scott, K. Motor control in a *Drosophila* taste circuit. *Neuron* **61**, 373–384 (2009).
10. Zimmermann, G. *et al.* Manipulation of an innate escape response in *Drosophila*: photoexcitation of acj6 neurons induces the escape response. *PLoS ONE* **4**, e5100 (2009).
11. Bellmann, D. *et al.* Optogenetically induced olfactory stimulation in *Drosophila* larvae reveals the neuronal basis of odor-aversion behavior. *Front. Behav. Neurosci.* **4**, 27 (2010).
12. Inagaki, H.K. *et al.* Visualizing neuromodulation *in vivo*: TANGO-mapping of dopamine signaling reveals appetite control of sugar sensing. *Cell* **148**, 583–595 (2012).
13. de Vries, S.E. & Clandinin, T. Optogenetic stimulation of escape behavior in *Drosophila melanogaster*. *J. Vis. Exp.* **71**, e50192 (2013).
14. Lima, S.Q. & Miesenbock, G. Remote control of behavior through genetically targeted photostimulation of neurons. *Cell* **121**, 141–152 (2005).
15. Hamada, F.N. *et al.* An internal thermal sensor controlling temperature preference in *Drosophila*. *Nature* **454**, 217–220 (2008).
16. Yizhar, O. *et al.* Neocortical excitation/inhibition balance in information processing and social dysfunction. *Nature* **477**, 171–178 (2011).
17. Lin, J.Y., Knutsen, P.M., Muller, A., Kleinfeld, D. & Tsien, R.Y. ReaChR: a red-shifted variant of channelrhodopsin enables deep transcranial optogenetic excitation. *Nat. Neurosci.* **16**, 1499–1508 (2013).
18. Scott, K. *et al.* A chemosensory gene family encoding candidate gustatory and olfactory receptors in *Drosophila*. *Cell* **104**, 661–673 (2001).
19. Boyden, E.S., Zhang, F., Bamberg, E., Nagel, G. & Deisseroth, K. Millisecond-timescale, genetically targeted optical control of neural activity. *Nat. Neurosci.* **8**, 1263–1268 (2005).
20. Nagel, G. *et al.* Channelrhodopsin-2, a directly light-gated cation-selective membrane channel. *Proc. Natl. Acad. Sci. USA* **100**, 13940–13945 (2003).
21. Nagel, G. *et al.* Light activation of channelrhodopsin-2 in excitable cells of *Caenorhabditis elegans* triggers rapid behavioral responses. *Curr. Biol.* **15**, 2279–2284 (2005).
22. Berndt, A., Yizhar, O., Gunaydin, L.A., Hegemann, P. & Deisseroth, K. Bi-stable neural state switches. *Nat. Neurosci.* **12**, 229–234 (2009).
23. Keene, A.C. & Masek, P. Optogenetic induction of aversive taste memory. *Neuroscience* **222**, 173–180 (2012).
24. Bianchi, D. *et al.* On the mechanisms underlying the depolarization block in the spiking dynamics of CA1 pyramidal neurons. *J. Comput. Neurosci.* **33**, 207–225 (2012).
25. Odden, J.P., Holbrook, S. & Doe, C.Q. *Drosophila HB9* is expressed in a subset of motoneurons and interneurons, where it regulates gene expression and axon pathfinding. *J. Neurosci.* **22**, 9143–9149 (2002).
26. Tayler, T.D., Pacheco, D.A., Hergarden, A.C., Murthy, M. & Anderson, D.J. A neuropeptide circuit that coordinates sperm transfer and copulation duration in *Drosophila*. *Proc. Natl. Acad. Sci. USA* **109**, 20697–20702 (2012).
27. Stockinger, P., Kvitsiani, D., Rotkopf, S., Tirián, L. & Dickson, B.J. Neural circuitry that governs *Drosophila* male courtship behavior. *Cell* **121**, 795–807 (2005).
28. von Philipsborn, A.C. *et al.* Neuronal control of *Drosophila* courtship song. *Neuron* **69**, 509–522 (2011).
29. Luan, H., Peabody, N.C., Vinson, C.R. & White, B.H. Refined spatial manipulation of neuronal function by combinatorial restriction of transgene expression. *Neuron* **52**, 425–436 (2006).
30. Pfeiffer, B.D. *et al.* Refinement of tools for targeted gene expression in *Drosophila*. *Genetics* **186**, 735–755 (2010).
31. Jenett, A. *et al.* A GAL4-driver line resource for *Drosophila* neurobiology. *Cell Rep.* **2**, 991–1001 (2012).
32. Pan, Y., Meissner, G.W. & Baker, B.S. Joint control of *Drosophila* male courtship behavior by motion cues and activation of male-specific P1 neurons. *Proc. Natl. Acad. Sci. USA* **109**, 10065–10070 (2012).
33. Yamaguchi, S., Desplan, C. & Heisenberg, M. Contribution of photoreceptor subtypes to spectral wavelength preference in *Drosophila*. *Proc. Natl. Acad. Sci. USA* **107**, 5634–5639 (2010).
34. Stavenga, D.G. Colour in the eyes of insects. *J. Comp. Physiol. A Neuroethol. Sens. Neural Behav. Physiol.* **188**, 337–348 (2002).
35. Hanai, S., Hamasaka, Y. & Ishida, N. Circadian entrainment to red light in *Drosophila*: requirement of Rhodopsin 1 and Rhodopsin 6. *Neuroreport* **19**, 1441–1444 (2008).
36. Clyne, J.D. & Miesenbock, G. Sex-specific control and tuning of the pattern generator for courtship song in *Drosophila*. *Cell* **133**, 354–363 (2008).
37. Kohatsu, S., Koganezawa, M. & Yamamoto, D. Female contact activates male-specific interneurons that trigger stereotypic courtship behavior in *Drosophila*. *Neuron* **69**, 498–508 (2011).
38. Yu, J.Y., Kanai, M.I., Demir, E., Jefferis, G.S. & Dickson, B.J. Cellular organization of the neural circuit that drives *Drosophila* courtship behavior. *Curr. Biol.* **20**, 1602–1614 (2010).
39. Dankert, H., Wang, L., Hoopfer, E.D., Anderson, D.J. & Perona, P. Automated monitoring and analysis of social behavior in *Drosophila*. *Nat. Methods* **6**, 297–303 (2009).
40. Tian, L. *et al.* Imaging neural activity in worms, flies and mice with improved GCaMP calcium indicators. *Nat. Methods* **6**, 875–881 (2009).

ONLINE METHODS

Construction of transgenic animals. Plasmids were constructed by standard DNA cloning and PCR methods. All PCR reactions were performed using PrimeStar HS DNA polymerase (Takara). Following amplification, all sequences were verified by DNA sequencing.

UAS-ChR2(H134R)::EYFP-2A-ChR2(H134R)::EYFP. A DNA fragment containing the ChR2(H134R) coding sequence, kindly provided by K. Deisseroth, and an intervening F2A sequence[12,41] were amplified by PCR using primers (5F-EcoRI-chr2, 3R-2a-YFP, 5F-2a-Chr2, 3R-Xba-YFP, 5F-2a and 3R-2a) and subcloned into pUAST vector in a tandem manner using restriction enzymes (see **Supplementary Table 4** for primer sequences). Several transgenic flies were created with different insertion sites. We picked the line that exhibited the strongest induction of PER when crossed to Gr5a-*GAL4*.

UAS-C1V1(T/T). A DNA fragment containing the coding sequence of C1V1(E122T/E162T)-TS-EYFP kindly provided by K. Deisseroth was amplified by PCR using primers (C1V1-f and C1V1-EGFP-r; see **Supplementary Table 4**). This PCR product was subcloned into the vector pJFRC2 (ref. 30) using SLIC cloning[42]. This vector was injected and integrated into attP40 and VK5 sites[30].

UAS-ReaChR, LexAop-ReaChR, UAS-FRT-*mCherry*-FRT-*ReaChR and LexAop*-FRT-*mCherry*-FRT-*ReaChR*. A DNA fragment containing the ReaChR::Citrine coding sequence was amplified by PCR using primers (ReaChR-f and ReaChR-citrine-r; see **Supplementary Table 4**). This PCR product was subcloned into pJFRC2 and pJFRC19 (ref. 30) using SLIC cloning[42] for UAS- and LexAop-driven versions, respectively. For the version containing an *FRT*–mCherry–Stop-*FRT* cassette, the *FRT* sequences (GAAGTTCCTATTCTCTAGAAAGTATAGGAACTTC) and ReaChR DNA fragments were subcloned together into pJFRC2 and pJFRC19 using SLIC cloning[42]. These vectors were injected and integrated into attP40, attP5 and VK5 sites[30].

Fly strains. UAS-ChR2 (ref. 5), UAS-dTrpA1 (ref. 15), UAS-GCaMP3.0 (ref. 40), Gr5a-*GAL4* (ref. 18) and BDP-*GAL4* (ref. 43) (empty promoter *GAL4*: an enhancerless *GAL4* containing a *Drosophila* basal promoter) were generously provided by A. Fiala, P.A. Garrity, L.L. Looger, K. Scott and G.M. Rubin, respectively. *fru-GAL4* (ref. 27), *fru-FLP*[38] and VT40556 *GAL4* (ref. 28) were kindly provided by B.J. Dickson. *hb9-GAL4* was obtained from Bloomington Stock Center (BL #32555). *Crz-GAL4* (ref. 26) and UAS-C128T[12] were previously created in the lab. All the transgenic flies created for this paper are summarized in **Supplementary Table 1**. These flies are available on request.

All experimental flies were maintained on a 12/12 h day-night cycle. Newly eclosed male flies were CO_2 anesthetized and allowed to recover for more than 3–7 d before behavioral tests at 25 °C. For dTrpA1 experiments, flies were raised at 18 °C. For experiments with Gr5a-*GAL4*, female flies were used; for all the other experiments, male flies were used.

Feeding of retinal. All-*trans*-retinal powder (Sigma) was stored in −20 °C as a 40 mM stock solution dissolved in DMSO (×100). 400 µl of sugar-retinal solution (400 µM all-*trans*-retinal diluted in 89 mM sucrose) was directly added to surface of solid food in food vials when larvae were at the first or second instar stage. After collection of newly eclosed flies, they were transferred into a vial containing food with 400 µM all-*trans*-retinal (food was heated and liquefied to mix the retinal evenly in the food). We found that larval feeding is not necessary, but it was performed for all the experiments in this paper to be consistent.

Behavioral setup. See **Supplementary Table 2** for a list of components used to assemble the behavioral setup. See **Supplementary Figure 1** for details of the setup and the behavioral chamber. In brief, high-power LEDs mounted on heat sinks were placed above the behavioral chamber to provide an illumination source (**Fig. 2a** and **Supplementary Fig. 1a**,**b**). The range of available light intensities in our setup is approximately 0.001–1 mW/mm^2 (note that intensity ranges are different for different LEDs; see **Supplementary Fig. 1d**). LED units were designed to be switchable to facilitate testing of different photostimulation wavelengths. The LEDs were controlled by an externally dimmable LED driver (700 mA, externally dimmable, Buckpuck DC driver with leads), and its output was adjusted using custom software controlling an Arduino Uno board (Smart Projects). The Arduino digital PWM output was converted into analog voltage using an RC filter (electronic low-pass filter composed of resistor and capacitor; RC LPF in **Fig. 2a**) containing a 200-Ω resistor and 1-µF capacitor to control the output current of the LED driver. Fly behavior was monitored using a CMOS camera equipped with an IR long-pass filter to avoid detection of light from the high-power LEDs. IR back light was used to visualize the behaving flies. Video capture and LED control were time locked using the Arduino Uno board. To time-stamp photostimulation trials in the videos, we placed an IR indicator LED, whose illumination was synchronized to that of the photostimulation LEDs, in the field of view of the camera. The temperature inside the behavioral chamber was minimally affected by the high-intensity photostimulation: after illumination using the highest available intensities of blue, green or red LEDs (1.1, 0.67 and 1.27 mW/mm^2, respectively) for 1 min, the biggest change in ambient temperature, detected using a thermocouple inserted into the chamber, was 0.7 °C.

Behavioral experiments and quantification of behaviors. For experiments to activate Gr5a-GRNs, nonstarved flies were mounted into 200-µl Pipetman tips as described previously[12]. Mounted flies were placed beneath high-power LEDs, and PERs were monitored using a video camera. Mounted flies were not placed in the behavioral chamber but placed at the same location as the wells of behavioral chamber in **Supplementary Figure 1b**. Bouts of PER were counted manually. A bout was defined as beginning when flies start extending their proboscis and ending when they retract the proboscis. Incomplete proboscis extensions were not counted. LEDs were used at maximum intensities in **Figures 1b**,**c** and **2d**,**e** (red, 1.1 mW/mm^2; amber, 0.22 mW/mm^2; green, 0.67 mW/mm^2; blue, 1.27 mW/mm^2). For **Figure 1b**, 100-ms photostimulation trials (1 Hz) were delivered (three trials), and flies showing more than one PER during this activation period were counted as responders. Fly genotype: w^-; Gr5a-*GAL4*(II); GR5a-*GAL4*(III)/UAS-ReaChR(VK5) (**Fig. 1b**–**g**); w^-; Gr5a-*GAL4*(II)/UAS-dTrpA1(II); GR5a(III)-*GAL4*/UAS-dTrpA1(III) (**Fig. 1h**).

To activate Crz neurons (**Fig. 2d**), males expressing each opsin in *Crz-GAL4* neurons were mounted dorsal side down on a glass

slide as previously described[26]. Flies were illuminated using the maximum available intensity of light for each type of LED, continuously for 1 min, while we monitored them from the ventral side using a video camera. The number of flies exhibiting ejaculation during light stimulation was manually counted.

For all other behavioral experiments, we used acrylic behavioral chambers (16-mm diameter) in a 2 × 4 array (**Fig. 2** and **Supplementary Fig. 1**) to monitor fly behavior. Unless otherwise indicated, chambers were photostimulated using the maximum intensity available for each LED, for 1 min using continuous illumination, while we monitored them with the camera from above. The number of flies showing continuous side walking during stimulation using the *hb9-GAL4* driver was manually counted (**Fig. 2d**,**f**). *fru-GAL4* neurons were activated in the same manner, and flies showing wing extension or paralysis phenotypes were counted manually (**Fig. 2d**,**g**). Paralysis was defined as the cessation of locomotion and loss of postural control. Flies that showed a weaker behavioral phenotypes (HB9, side walk; Fru, wing extension) at the onset of photostimulation, but that were paralyzed before the 1-min stimulation was terminated, were counted as paralysis (**Fig. 2f**,**g**).

Wing extension evoked by activation of P1 or pIP10 neurons were tested in solitary males in the absence of female flies. The wing extension was manually scored (**Figs. 2**–**5**). Grooming (rapid wing movements while touching with hind leg) was excluded. A bout was defined as starting when flies begin to increase the wing angle and ending when they stop decreasing it.

In order to fit the data into a sigmoidal curve, sigmoid interpolation was performed. The sigmoid curves were defined as follows

$$F_{\text{behav}} = \frac{1}{1 + e^{-\alpha \log_2 \frac{X}{X_{50}}}}$$

where F_{behav} is the fraction of flies showing the behavior, X is the light intensity (**Figs. 3f**, **4c** and **5c**) or frequency (**Fig. 2e**), X_{50} is the light intensity (**Figs. 3f**, **4c** and **5c**) or frequency (**Fig. 2e**) where 50% of flies show the behavior, and α is the slope of the sigmoid curve.

On the basis of the experimentally measured quantities (X and F_{behav}), X_{50} and α were chosen to best fit the data. For all experimental data, polynomial curve fitting—which finds the coefficients that fit the data by the least-squares method—was calculated with Matlab (MathWorks). Goodness of fit was tested by two-way ANOVA between the sigmoidal curve and the actual PER response curve, which indicated a good fit for all cases ($P < 0.05$, two-way ANOVA). The X_{50} is shown as 50% point in the figures (**Figs. 2e**, **3f**, **4c** and **5c**).

Measurement of light intensity. A photodiode power sensor (S130VC, Thorlabs) was placed at the location of the behavioral chamber but in the absence of the chamber. The peak wavelength of each LED (red, 627 nm; amber, 590 nm; green, 530 nm; blue, 470 nm) was measured at different voltage inputs. Measurements were repeated four times and averaged. The baseline intensity of each wavelength before LED illumination was subtracted. Note that light intensity can drop during stimulation at high input voltages. In this study, intensity after 10 s of stimulation was measured.

Measurement of penetrance of different wavelengths of light through the fly cuticle. The proboscis of a female adult fly was removed, and a 10-µm multimode optic fiber (NA, 0.1; Thorlabs) was inserted into the brain through the window. The amount of light entering the optic fiber inside or outside the fly was measured using a power meter (Model 1931, Newport). Penetrance was calculated as the amount of light that entered the optic fiber inside the fly divided by the amount of light measured outside the fly. The long axis of the optic fiber was always aligned with the light source. Different wavelengths of high power LEDs (470 nm, 530 nm, 590 m, 627 nm) were used as light sources.

Fly histology. All fixation and staining procedures were performed at 4 °C in PBS unless otherwise specified. Dissected brains were fixed in 4% formaldehyde in PEM (0.1 M PIPES, pH 6.95, 2 mM EGTA, 1 mM $MgSO_4$) for 2 h. After three 15-min rinses with PBS, brains were incubated with primary antibodies overnight. Following three 15 min rinses with PBS, brains were incubated with secondary antibody overnight. Following three 15-min rinses, brains were incubated in 50% glycerol in PBS for 2 h and cleared with Vectashield (Vector Labs). All procedures were performed at 4 °C. A FluoView FV1000 Confocal laser scanning biological microscope (Olympus) with a 30×/1.05-NA silicone oil objective (Olympus) was used to obtain confocal serial optical sections. The antibodies used for **Supplementary Figure 2a**,**d** were anti-GFP, rabbit polyclonal antibody unconjugated (A11122, Invitrogen) and Alexa Fluor 488 donkey anti-rabbit IgG(H+L) (A11008, Invitrogen). Both of the antibodies were diluted to 1/300. Expression of mCherry in **Supplementary Figure 2d** was monitored using native fluorescence without antibody staining.

FluoRender software[44] (http://www.sci.utah.edu/software/13-software/127-fluorender.html) was used to make 3D image reconstructions. To measure the expression levels of ReaChR::Citrine in P1 neurons in **Figure 6d**, the native fluorescence of Citrine in different specimens was monitored using the same intensity of laser power (470 nm) and PMT voltage. Signal intensity was quantified in ImageJ (http://rsbweb.nih.gov/ij/).

Calcium imaging. Two-photon imaging was performed on an Ultima two-photon laser-scanning microscope (Prairie Technology) with an imaging wavelength of 925 nm (**Fig. 6**). To filter out autofluorescence of the brain and light from the amber stimulation LED (for ReaChR activation), we used a 500/20 nm (center wavelength/bandwidth) band-pass filter (Chroma) in the emission pathway to detect the GCaMP3 fluorescence. With this laser and filter setting, fluorescence emissions from the Citrine tag (on ReaChR) were not detectable by our PMT. This was confirmed by examination of P1-GAL4;UAS-ReaChR::Citrine flies (the flies without GCaMP3.0), which exhibited no fluorescence signal under our imaging conditions. Therefore, the detected fluorescence signals are purely from GCaMP3.0. The scanning resolution was 128 × 128 pixels, dwell time per pixel was 8 µsec and the optical zoom was 4×. The scanning speed was ~10 Hz. The excitation intensity of the two-photon laser was varied among samples depending on the level of GCaMP3.

doi:10.1038/nmeth.2765

In both cases, a 40×/0.80-NA water-immersion objective (Olympus) was used for imaging. A high-power amber LED (590 nm) collimated with an optic fiber (M590F1, Thorlabs) was used as a light source to activate ReaChR. To narrow the bandwidth of the LED output, we connected the optic fiber to a fiber optic filter holder (World Precision Instruments) equipped with 589/10 nm (center wavelength/bandwidth) band-pass filter (Edmund optics). A 200-µm core multimode optic fiber (NA, 0.39; FT200EMT, Thorlabs) was used to deliver the light from the fiber optic holder to the brain. One side of the optic fiber was custom-made to be a bare tip (Thorlabs) and was dipped into the saline imaging bath and placed 430 µm away from the brain. A 10×/0.30-NA water-immersion objective (Olympus) was used to locate the brain and align the optic fiber. The distance between brain and the fiber was measured with an objective micrometer (Olympus). We set the light intensity to be 170 µW at the tip of optic fiber. Thus, at a distance of 430 µm from the tip of a 0.39-NA optic fiber, the light power is calculated to be approximately 1.7 mW/mm^2 at the brain surface (the size of the light spot should be approximately 0.10 mm^2 at the brain). In addition to the PMT used to monitor GCaMP emissions, we used another PMT to monitor the 590-nm ReaChR activation light. This was to ensure that the intensities of 590-nm light were comparable between samples.

To prepare the brain for imaging, we used an *ex vivo* prep. After briefly anesthetizing a fly on ice, the brain was dissected out using a sharp forceps into a 35-mm plastic Petri dish (35 3001, Falcon) containing *Drosophila* imaging saline (108 mM NaCl, 5 mM KCl, 2 mM $CaCl_2$, 8.2 mM $MgCl_2$, 4 mM $NaHCO_3$, 1 mM NaH_2PO_4, 5 mM trehalose, 10 mM sucrose, 5 mM HEPES, pH 7.5)[45]. The fat body, air sacs and esophagus were gently removed to give a clear view of the brain and to minimize its movement. The brains were attached to the bottom of the plate by static. The saline was changed once after dissection to remove debris. Calcium imaging was performed within 10–15 min after the dissection to ensure that the brains were healthy.

Electrophysiology. The tip recording method was used to record the electrophysiological responses of labellar taste neurons[46]. Briefly, the fly was mounted and immobilized for recording by inserting a pulled glass capillary (BF150-86-10, Sutter Instruments) from the dorsal surface of the thorax to the tip of the labellum, passing through the cervical connective and the head. The mounting glass capillary was filled with recording solution (7.5 g/L NaCl, 0.35 g/L KCl, 0.279 g/L $CaCl_2{\cdot}2H_2O$ and 11.915 g/L HEPES (Sigma-Aldrich)) and served as a ground electrode. Another glass capillary, pulled to a tip diameter of 10–20 µm and filled with 30 mM tricholine citrate (TCC; Sigma-Aldrich), as an electrolyte, was used for recording the electrophysiological responses of the gustatory neurons innervating this sensillum. All the recordings were obtained from L7 sensilla. The recordings were made using a MultiClamp 700B amplifier and Digidata 1440A A/D converter (Molecular Devices). The recorded data were sampled at a rate of 10 kHz, filtered (band-pass filter between 100 Hz and 3 kHz) and stored on a PC hard drive using Clampex 10 software (Molecular Devices). The data were analyzed by sorting the action potentials and measuring their frequency within the indicated time windows using Clampfit software (Molecular Devices).

For PER activation experiments, a high-power amber LED (590 nm) collimated with an optic fiber (M590F1, Thorlabs) was used as a light source to activate ReaChR. For delivering light to the labellum, a 200-µm core multimode optic fiber with bare end (NA, 0.39; Thorlabs) was used. The distance of optic fiber from the labellum was set to be 540 µm using a micrometer. The estimated light intensity at the labellum was approximately 1.0 mW/mm^2.

To activate TrpA1 (**Fig. 1h**), we used a custom-made heat source. In brief, the heat source is a small piece of thermistor (2K Bead Thermistor, Fenwal) that emits heat in proportion to the electrical current passed through it. The distance of the heat source from the labellum was set to be 540 µm using a micrometer. The temperature at this distance was measured using a thermocouple (Omega) (top panel in **Fig. 1h**).

41. Donnelly, M.L. *et al.* The 'cleavage' activities of foot-and-mouth disease virus 2A site-directed mutants and naturally occurring '2A-like' sequences. *J. Gen. Virol.* **82**, 1027–1041 (2001).
42. Li, M.Z. & Elledge, S.J. Harnessing homologous recombination *in vitro* to generate recombinant DNA via SLIC. *Nat. Methods* **4**, 251–256 (2007).
43. Pfeiffer, B.D. *et al.* Tools for neuroanatomy and neurogenetics in *Drosophila*. *Proc. Natl. Acad. Sci. USA* **105**, 9715–9720 (2008).
44. Wan, Y., Otsuna, H., Chien, C.B. & Hansen, C. An interactive visualization tool for multi-channel confocal microscopy data in neurobiology research. *IEEE Trans. Vis. Comput. Graph.* **15**, 1489–1496 (2009).
45. Wong, A.M., Wang, J.W. & Axel, R. Spatial representation of the glomerular map in the *Drosophila* protocerebrum. *Cell* **109**, 229–241 (2002).
46. Hodgson, E.S., Lettvin, J.Y. & Roeder, K.D. Physiology of a primary chemoreceptor unit. *Science* **122**, 417–418 (1955).